Ion-implantation- and thermal-anneal-induced intermixing in thin Si/Ge superlattices

W. Freiman and R. Beserman
Solid State Institute and Physics Department, Technion-Israel Institute of Technology, Haifa, Israel

Yu. L. Khait and M. Shaanan
Solid State Institute, Technion-Israel Institute of Technology, Haifa, Israel

K. Dettmer and F. R. Kessler
Institute of Semiconductor Physics and Optics, Technical University, Braunschweig, Germany
(Received 18 September 1992; revised manuscript received 1 March 1993)

Superlattices (SL's) composed of thin Si and Ge layers ($Si_{12}Ge_{12}$, $Si_{19}Ge_9$) have been implanted with As, Ge, and Ga ions with doses ranging from 1×10^{13} to 1×10^{14} ions cm^{-2}, and thermally annealed at 600 °C for 30 min. The disordering and the intermixing of these SL's have been studied by the Raman-scattering technique and model calculations. The damage created by ion implantation has been estimated using TRIM simulations and a model. We found that when a thin symmetric $Si_{12}Ge_{12}$ SL was rendered amorphous by ion implantation at high doses $\geq 5\times10^{13}$ ions cm^{-2}, a mixed $Si_{0.5}Ge_{0.5}$ material was produced by thermal annealing, but the crystalline structure of the asymmetric $Si_{19}Ge_9$ SL equally disordered and annealed returns to a different SL structure with very little intermixing between the layers. Using a kinetic model, we calculated the interdiffusion coefficients and it was found that the recrystallization of the Ge layer is a fast process but that of the Si one is slow with respect to the time needed for intermixing. As a result, Ge diffuses mainly in disordered Si layers and Si in ordered Ge layers. In order to explain our experimental results, we equate the diffusion of Si into crystalline Ge to that of Ge into amorphous Si to minimize the effect of interlayer stress. Model calculations explain the difference in behavior between the two types of SL's, and are in good agreement with the Raman data.

I. INTRODUCTION

The ability to alter locally the electronic and optical properties of superlattices (SL's) has been used for band-gap engineering with significant applications in optoelectronic device technology.[1–4] Impurity-induced disordering of heterostructures and SL's has been induced by the diffusion of active impurities.[5,6] It has been demonstrated that the implantation of Si into GaAs/AlAs SL's creates mixing at depths larger than four times the projected range, while in the region of maximum implantation damage, mixing is inhibited due to dislocation loops.[7]

In GaAs/AlAs SL's, the diffusion of Si is highly correlated with the displacement of Al.[7] The diffusion of dopant impurities in GaAs/$Ga_{1-x}Al_xAs$ SL's has been explained using a kick-out mechanism in which interstitial Ga^{++} governs the Ga self-diffusion.[8]

The picture for III-V SL's and quantum wells is that implantation damage alone followed by thermal annealing is sufficient for layer intermixing, but the dopant-induced intermixing is a completely different process, where the dopant impurities ensure a faster disordering of the layered structure.[9]

Thin Si_mGe_n strained-layer superlattices (SLS's) have recently attracted considerable interest because of the possibility to obtain a quasidirect band gap.[10,11] Support for a direct band-gap material has been given by various authors,[12,13] but this claim has been questioned; different possibilities for a faulty interpretation exist: incorrect interpretation of photoluminescence spectra due to the role of band-edge luminescence,[14] and impurities or point defects inherited from low-temperature epitaxy.[15,16] The stability of these highly strained SL's has become an important issue, and the diffusion between Si and Ge has been widely studied as a function of thermal treatment.[17–20]

It is then of interest to study the intermixing process in the simplest possible SL structure or heterostructures. In this paper, we shall study the kinetics of the intermixing processes of Si/Ge SL's which are damaged by ion implantation and thermally annealed. We have already shown that the nature of the implanted ion does not influence significantly the intermixing process.[21] Thus here we only report on As-implanted samples.

The kinetics of processes caused by ion bombardment and thermal annealing in SL's composed of very thin layers differ substantially from their counterparts in thick-film structures. One of the main causes of these differences is associated with the fact that low-energy recoils and diffusing atoms of one kind (Si atoms) need to pass small distances of a few interatomic spacings to appear in neighboring layers composed of another type of particles (Ge atoms). Another difference results from the stress which exists between adjacent layers. These factors lead to (a) a marked intermixing in the thin-layer SL's during the implantation process, and (b) a considerable intermixing caused by thermal annealing during relatively short-time intervals (30 min) at moderate temperatures (600 °C). The above facts are confirmed by our experimental studies and by TRIM computer cascade simulations and model calculations. The paper is organized as

follows: In Sec. II, disordering and intermixing caused by ion implantation in Si/Ge SL's composed of thin layers are considered. Experimental results are described in Sec. III. The kinetics of reordering, interdiffusion, and intermixing during the thermal annealing are considered in Sec. IV. A conclusion is given in Sec. V.

II. DISORDER CREATED BY ION IMPLANTATION IN THIN Si/Ge SL's

Intermixing of Si/Ge SL's caused by ion implantation followed by thermal annealing is clearly the result of two different phenomena.

(1) Damage in the SL structure created by the implantation of foreign ions which lead to a partial intermixing of the Si and Ge layers.

(2) Intermixing due to the diffusion of Si and Ge atoms under the influence of thermal heating.

The two phenomena differ considerably from each other; each of them is characterized by its own specific kinetics. We shall consider the two phenomena separately; first we evaluate the intermixing due to ion implantation, and afterward we shall estimate the effect of temperature on disordered and ordered structures.

In order to shed light on the migration of the recoils produced during the implantation process, use was made of the TRIM program.[22] This program calculates, using the Monte Carlo technique, the penetration of ions with a given energy into homogeneous or layered targets. It takes into consideration the energy losses of the ion due to elastic collisions with the target atoms and interactions with the target electrons. The TRIM85 version used in this study was modified so as to be able to deal with thin layers. The output of the modified program is (a) the depth distribution of the recoils produced during the implantation process, and (b) the spatial distribution of Si (or Ge) atoms in neighboring Ge (or Si) layers which is associated with intermixing caused by ion bombardment (Figs. 1 and 2).

First, the preliminary auxiliary calculations were carried out in order to see where the maximum damage occurs. A simulation was performed for the following structure: a Si cap layer of thickness of 500 Å, a Si/Ge binary mixture (alloy) of thickness of 1000 Å representing the SL, and a thick layer of Si (the substrate). The implanted species were As ions of an energy of 220 keV. TRIM calculations for the auxiliary system indicated that the maximum damage occurred at a depth of about 750 Å, i.e., at a depth of about 250 Å within the Si/Ge binary system replacing the SL. At this depth, the energy of the incoming As ions was about 142 keV. The second stage of TRIM calculations for ion implantations in the Si/Ge SL was carried out in accordance with the preliminary results. In the calculation, As ions of 150-keV energy were implanted in the following two structures.

(1) The symmetric SL composed of five pairs of Si and Ge layers, each of equal thickness, composed of 12 atomic layers.

(2) The asymmetric SL composed of five pairs of Si and Ge layers of different thickness, the Si layer composed of 19 atomic layers and the Ge layers of nine atomic layers.

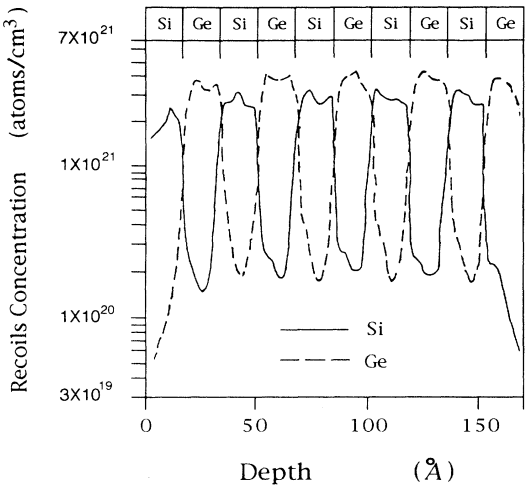

FIG. 1. Spatial distribution of the recoil concentration in the symmetrical $Si_{12}Ge_{12}$ SL obtained from a TRIM computer simulation of As ion implantation for a dose of 5×10^{13} ions cm^{-2}.

The results of the TRIM calculations for the two types of SL's described above, which were implanted with dose of 5×10^{13} ions cm^{-2}, are given in Figs. 1 and 2. These calculations show that approximately equal damage is produced in the Si and Ge layers by the ion bombardment in both kinds of SL's. On the other hand, the spatial distributions of Si and Ge atoms and therefore the intermixing caused by the ion bombardment are different in the Si and Ge layers of the symmetrical and the asymmetrical SL's. These differences can be summarized as follows: In both kinds of SL's, the concentration of foreign Si or Ge atoms in Ge or Si layers is relatively high at the interface and decreases substantially in the middle of these layers. The concentration of Si atoms in Ge layers decreases from about 1% (or 3%) at the Si-Ge-layers in-

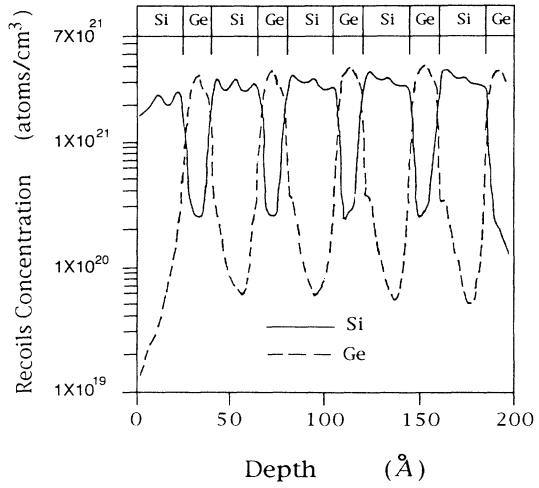

FIG. 2. Spatial distribution of the recoil concentration in the asymmetrical $Si_{19}Ge_9$ SL obtained from a TRIM computer simulation of As ion implantation for a dose of 5×10^{13} ions cm^{-2}.

terface to about 0.4% (or 0.75%) in the middle of the Ge layers in the symmetric (or asymmetric) SL. The concentration of Ge atoms in the Si layers decreases from about 2% (or 4%) at the Ge-Si interface down to about 0.12% (or 0.18%) in the middle of the Si layers.

Thus the TRIM calculations show significant intermixing inside the Ge layers and a lower degree of intermixing in the Si layers caused by ion bombardment in both SL's. The substantial degree of intermixing caused by ion implantation in Si_mGe_n SL's is promoted by a very small thickness of the SL layers which are defined by

$$\Delta l_{Si}=m\Delta d, \quad \Delta l_{Ge}=n\Delta d \ . \tag{1}$$

Here Δd is the thickness of the atomic monolayer, $m=n=12$ in the symmetrical case and $m'=19$ and $n'=9$ in the asymmetrical case. The ion bombardment creates a large number of Si and Ge recoils of relatively small energy, each having a "stopping length" of one or a few interatomic distances d. At the same time, the low-energy Si (or Ge) recoil atoms should pass distances

$$\Delta z \leq \frac{m\Delta d}{2} \approx 6\Delta d \tag{2}$$

or

$$\Delta z' \leq \frac{m'\Delta d}{2} \approx 10\Delta d \quad \text{and} \quad \Delta z'' \leq \frac{n'\Delta d}{2} \approx 5\Delta d \tag{3}$$

to appear in the neighboring Ge (or Si) layers of different compositions, in $Si_{12}Ge_{12}$ and $Si_{19}Ge_9$ SL's, respectively. Hence one can see that "stopping length" l of the Si and Ge recoils is of the order of the distances Δz (or $\Delta z'$ or $\Delta z''$). This leads to the substantial intermixing in the Si_mGe_n SL's during ion implantation which is found in our TRIM calculations. It should be pointed out that these calculations do not take into account some dynamic effects such as atomic diffusion and short-lived hot spots induced by the ion bombardment, which can influence the degree of intermixing and disordering in the SL's composed of thin layers. Among the disregarded effects, we can point out the following.

(i) The ion bombardment generates interstitial atoms which have rather high diffusion coefficients D_i even at room temperature due to low activation energies ΔE_i.[23–26] In the system of thin layers, the mean free path $\lambda_i \approx (N_v\sigma)^{-1}$ of the interstitials with respect to their recombination with vacancies (of concentration per cm^3 N_v) is comparable to or larger than Δl_{Si} or Δl_{Ge} [Eq. (1)], where σ is the recombination cross section. As a result, interstitial Si (or Ge) atoms can penetrate deeply into neighboring Ge (or Si) layers.

(ii) A high concentration of vacancies created by ion bombardment[23–26] can enhance considerably the diffusion coefficient as shown in Refs. 27 and 28, in connection with crystallization and diffusion in a-Si. These processes promote intermixing in the Si_mGe_n SL's during ion implantation. One can expect that intermixing in Ge layers should be larger than that in Si layers since the activation energy for Si diffusion in Ge is substantially lower than the activation energy for diffusion of Ge in Si.

(iii) Ion bombardment produces a nonequilibrium concentration of excited and mobile carriers. The interaction of these carriers with diffusing atoms enhances substantially the diffusion coefficient at low temperature.[27–30]

The processes mentioned above can highly increase the degree of intermixing obtained from the TRIM calculations up to values not low compared to the maximum concentration of Si (or Ge) recoils in the Si (or Ge) layers. Thus one can expect that under favorable conditions (see below), the degree of intermixing during ion implantation can reach values of about 5–10 % for the dose $\approx 5\times10^{13}$ ions cm^{-2}. In particular, fast-diffusing Si (or Ge) interstitials can contribute substantially to intermixing when the following condition is satisfied:

$$\lambda_i \approx (N_v\sigma)^{-1} > \frac{\Delta l_{Si}}{2} \quad \text{or} \quad \frac{\Delta l_{Ge}}{2} \ . \tag{4}$$

The better this condition is satisfied, the larger a degree of intermixing one can expect. For the asymmetrical case when $\Delta l_{Si} \approx 2\Delta l_{Ge}$ and $\lambda_i \approx 25$ Å (for $N_v \approx 10\%$ N and $\sigma \approx 10^{-15}$ cm^{-2}), one can expect larger intermixing of Si in the Ge layers than of Ge atoms in the Si layers. Faster diffusion of Si atoms in Ge (compared to that of Ge in Si) also favors larger intermixing of Si in the Ge layers both in the symmetrical and asymmetrical cases.

At doses of 5×10^{13} ions cm^{-2}, the disordering and amorphization in the Si and Ge layers do not differ substantially in both SL's. Raman spectroscopy studies of the SL's after the implantation (but before annealing) confirm the conclusions mentioned above.

III. EXPERIMENTAL RESULTS

Molecular-beam epitaxy of Si_xGe_{1-x} buffer layers and Si_mGe_n SL films was performed in a Balzers ultrahigh vacuum (UHV) unit, UMS 500. The [001] Si wafers were chemically precleaned and deoxided in UHV at high temperature. The substrate temperature during growth was held at 350 °C. The $(Si_{12}Ge_{12})_{33}$ SL with an upper Si capping layer 490 Å thick, was grown on a 200-Å-thick $Si_{0.56}Ge_{0.44}$ buffer layer.[21] The $(Si_{19}Ge_9)_{30}$ SL with a 170-Å Si capping layer was grown on a 1200-Å-thick $Si_{0.70}Ge_{0.30}$ buffer layer.[31]

The symmetric SL $(Si_{12}Ge_{12})$ has been implanted with As, Ga, and Ge ions with doses between 1×10^{13} and 1×10^{14} ions cm^{-2}. A thermal treatment at $T_a=600$ °C during $t_a=30$ min in vacuum was carried out to reduce the damage created during ion implantation and to intermix the Si and Ge layers. The Raman measurements were performed at room temperature in the backscattering geometry, using the 4579-, 4880-, and 5145-Å lines of an Ar^+ laser, where the first laser wavelength has a relatively small penetration depth and probes the upper layers of the SL structure and its capping layer. With the 5145-Å wavelength, the laser light penetrates through the capping layer, through the entire SL, and reaches the Si substrate. The 4880-Å wavelength on the other hand, analyzes mainly the depth where the SL's Si-Ge layers are located, as seen in Fig. 3. The arrows show the depth where the laser is reduced to 0.3 of its initial penetrating intensity. The laser light power was 200 mW, focused on

a spot of about 200 μm^2. Scattered light was analyzed with a Spex 1403 double spectrometer. The distribution of the damage produced by the implanted ions is also shown in Fig. 3. The laser penetration depth can be estimated by

$$I = I_0(1-R)\exp(-2\gamma d) , \quad (5)$$

$$\gamma = \frac{2\pi k}{\lambda_0} , \quad (6)$$

where I is the scattered intensity and I_0 is the laser intensity. R is the reflectivity. γ defines the attenuation of the laser in the direction of the wave propagation. k is the imaginary part of the complex refractive index: $N = n - ik$, and depends on the laser frequency; λ_0 is the wavelength of the laser in free space. The extinction coefficient k of Si and Ge for various wavelengths of the laser is obtained from the literature.

In Ref. 21, some of our results were reported. We showed that the damage created by the ion implantation of the heavy atoms As, Ge, and Ga was important when the implantation dose (ID) is greater than 10^{13} ions cm^{-2}. The SL's become amorphous (no crystalline Raman line) when the ID of As $\geq 2\times10^{13}$ ions cm^{-2}. After thermal annealing at 600 °C for 30 min, the crystalline structure of the damaged SL is restored. After annealing, the Raman spectrum of the original unimplanted SL is similar to that obtained before annealing, because the activation energy of Si and Ge in the Ge and Si layers, respectively, is high in the absence of defects (see Table I). In Fig. 4(a), we see the typical four-mode spectrum of the unimplanted and annealed SL, with the Ge-Ge, Ge-Si, and Si-Si vibrations of the SL layers and the Si-Si vibration of the substrate (306, 405, 505, and 520 cm^{-1}, respectively). A comparison between these frequencies and the Ge and Si bulk ones (300 and 520 cm^{-1}, respectively) shows downward and upward shifts of the Si-Si and Ge-Ge peaks, respectively, which are due to the presence of tensile and compressive strains in the single Si and Ge layers, respectively, of the SL. In Figs. 4(b)–4(e), we show the Raman spectra excited by the 5145-Å laser line of the samples implanted with As doses ranging from 10^{13} to 10^{14} ions/cm^2 after annealing.

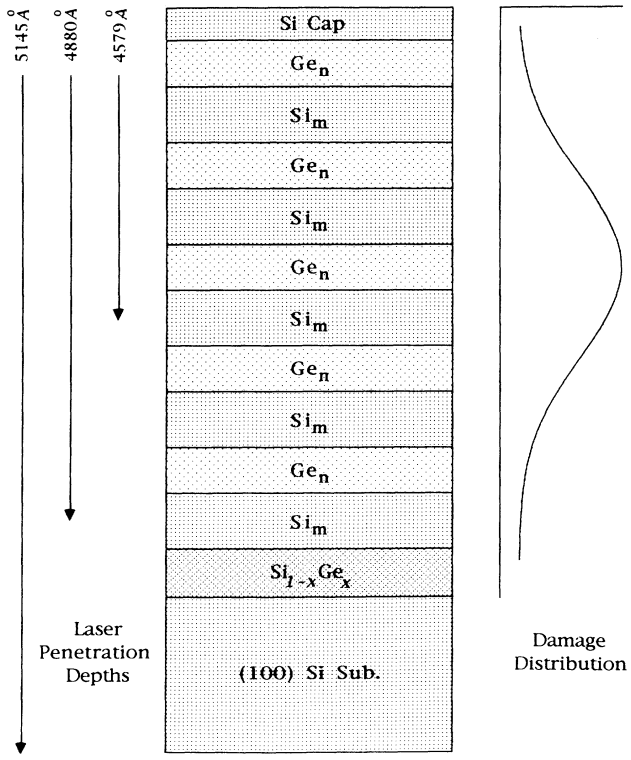

FIG. 3. The five-period superlattice structure and the spatial distribution of the damage caused by ion implantation, obtained from TRIM calculations with different laser wavelength penetration depths.

After implantation and annealing, two processes can occur.

(i) The release of the strain which results in a downward shift of the Ge-Ge frequency and in an upward shift of the Si-Si one.

(ii) Intermixing between the Si and Ge layers which is characterized by (a) a downward shift of the Ge-Ge frequency ≤ 300 cm^{-1}. (b) The Raman intensity ratio I(Ge-Ge)/I(Si-Si) tends toward 1. (c) A downward shift of the Si-Si frequency (as opposed to the upward shift which results from strain release).

After thermal annealing, and when the implantation dose is lower than 2×10^{13} ions cm^{-2}, i.e., as long as the implanted SL retains some trace of crystalline structure, the dominant factors are the following.

(i) A downward shift of the Ge-Ge frequency due to a release of strain between adjacent layers (the frequencies are above 300 cm^{-1}).

(ii) A relative increase of the Si-Ge intensity with respect to the Ge-Ge one which shows that some intermixing between the layers takes place.

(iii) The Si-Si peak is broadened and not well defined by the appearance of the Raman peaks characteristic of the Si-Si vibrations in the Si and Ge layers. This will be discussed below in more detail.

We want to point out that, after implantation and recrystallization, the absorption coefficient of the SL decreases when the ID increases, because the structure of

TABLE I. Diffusion constants for diffusion of Si and Ge into crystallized (c) and amorphous (a) structures.

	D_0 ($cm^2 s^{-1}$)	ΔE (eV)	D (873 K) ($cm^2 s^{-1}$)	Ref.
Ge⟹a-Ge Si⟹a-Ge	10^{-6}	1.6	5.5×10^{-16}	33
Ge⟹c-Ge Si⟹c-Ge	18.5	3.07	3.2×10^{-17}	34
Ge⟹a-Si Si⟹a-Si	10^{-3}	2.5	3.45×10^{-18}	39
Ge⟹c-Si Si⟹c-Si	2×10^{3}	4.8	3.43×10^{-25}	34

the SL becomes more homogeneous and more like that of a mixed crystal, as seen from the increase of the Raman intensity of the Si substrate peak at 520 cm^{-1}. Very little change, if any, takes place when the ID increases from 5×10^{13} to 10^{14} ions cm^2 [Figs. 4(d) and 4(e)]. The phonon vibration values are the frequencies of the $Si_{0.5}Ge_{0.5}$ mixed polycrystal.[32]

With a 4880-Å laser wavelength, the depth under study is mainly that of the damaged SL layers. Figure 5 shows a detailed study of the 435–525-cm^{-1} frequency range, which contains the different Si-Si vibrations. Before implantation, we can see the vibrational frequencies of the substrate's Si atoms at 520 cm^{-1}, of the capping layer at 509 cm^{-1}, and of the SL Si vibrations at 502 cm^{-1}. After implantation of 1×10^{13} ions cm^{-2} and annealing [Fig. 5(b)], the Si-Si peak of the Si SL layers is shifted toward lower frequencies. The broad shoulder at ~485 cm^{-1} [Fig. 5(b)] can be related to the Si-Si vibrations of the mixed Si_xGe_{1-x} layers which replace the former pure Ge layers. The mixed Si_yGe_{1-y} layers which replace the former pure Si layers give rise to a Raman peak around 500 cm^{-1}. Both x and y are depth dependent with $(1-y)<x<0.5$. The values x and $1-y$ are different because the Si atoms penetrate more easily into the Ge layers than the Ge atoms into the Si layers. During the annealing process, this leads to $(1-y)<x$, and to Si_yGe_{1-y} layers which are thinner than the original Si layers and than the Si_xGe_{1-x} ones (formerly the Ge layers). With increasing ID, the difference between x and $1-y$ tends to decrease, and for high enough ID, we get a mixed-crystal $Si_{0.5}Ge_{0.5}$.

We follow this evolution experimentally in Fig. 5. For a low implantation dose, the main contribution to the Raman spectrum comes from the Si-Si vibration of the Si_yGe_{1-y} layers [Fig. 5(b)]. In Fig. 5(c), we can see the two Si-Si vibrations of Si_xGe_{1-x} and Si_yGe_{1-y} (with $(1-y)<x$) at 490 and 500 cm^{-1}, respectively. These two

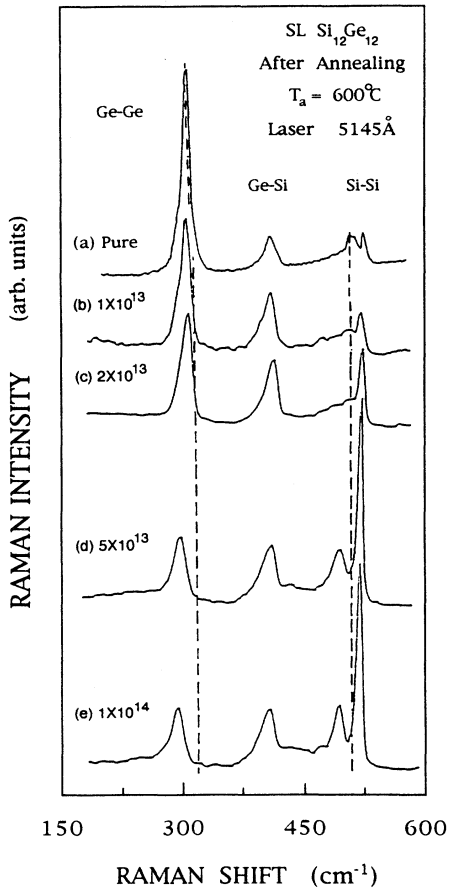

FIG. 4. Raman spectra of $Si_{12}Ge_{12}$ after As implantation and thermal annealing at 600 °C for 30 min with dose of (a) as grown, (b) 1×10^{13}, (c) 2×10^{13}, (d) 5×10^{13}, and (e) 1×10^{14} As ions cm^{-2}. The incident laser wavelength was 5145 Å.

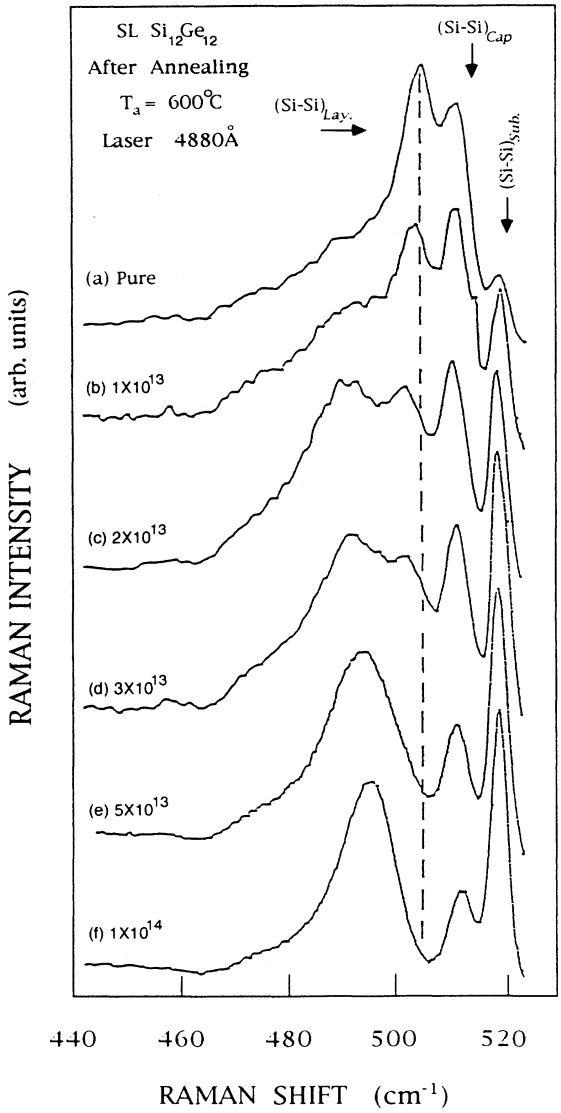

FIG. 5. Raman spectra of $Si_{12}Ge_{12}$ after As implantation and thermal annealing at 600 °C for 30 min with dose of (a) as grown, (b) 1×10^{13}, (c) 2×10^{13}, (d) 3×10^{13}, (e) 5×10^{13}, and (f) 1×10^{14} As ions cm^{-2}. The incident laser wavelength was 4880 Å.

peaks merge into a broad band when ID $\geq 5\times10^{13}$ ions cm^{-2}. The broad Raman peak centered around 490 cm^{-1} [Figs. 5(c) and 5(d)] is the broadened frequency of the Si-Si vibration in the Si_xGe_{1-x} layer. This broadening is the result of the gradient of the Si concentration inside the pure ex-Ge layers. When the dose is $\geq 5\times10^{13}$ ions cm^{-2}, the layers are well mixed and we get a well-defined narrow Si-Si peak at 493 cm^{-1}, characteristic of polycrystalline $Si_{0.5}Ge_{0.5}$, seen in Figs. 5(e) and 5(f). We want to emphasize that gradients of x and y take place in both mixed layers. At the interface their values are close to those of the mixed monoatomic layer, and they decrease toward the middle of the layer. The thinning of the Si_yGe_{1-y} layers with respect to the Si_xGe_{1-x} can be seen in Figs. 5(b)–5(d). The intensity ratio between the Si-Si vibrations of the two layers decreases with the emerging of a strong Si-Si vibration of the Si_xGe_{1-x} layers. Figure 6 summarizes our view on the evolution of the intermixing process as a function of ID. This figure is a schematic diagram which explains the structure differences between the ex-Si and the ex-Ge layers as a function of ID after thermal annealing in the symmetric SL. Figure 6(a) shows the SL before implantation. For implantation at low ID followed by thermal annealing, the layers are partially mixed with $(1-y)<x$ [Fig. 6(b)]. In Fig. 6(c), we see the mixed crystal when the

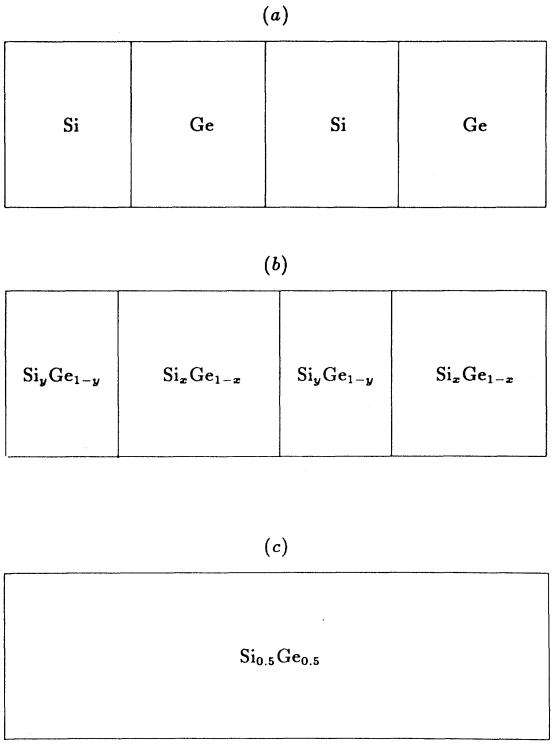

FIG. 6. The intermixing process in the symmetric $Si_{12}Ge_{12}$ SL. (a) The unimplanted sample; (b) intermixing of the layers after the implantation with the lower doses of 1×10^{13}–3×10^{13} ions cm^{-2}, followed by an annealing process where $(1-y)<x<0.5$; and (c) the complete intermixing of the symmetric sample after the implantation with the higher doses of 5×10^{13}–1×10^{14} ions cm^{-2} and annealing, where $x=y=0.5$.

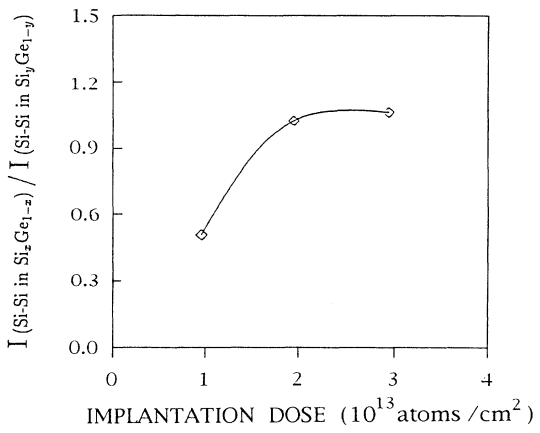

FIG. 7. The intensity ratio between the Si-Si Raman peaks originated in the Si_xGe_{1-x} and Si_yGe_{1-y} layers in the symmetric $Si_{12}Ge_{12}$ SL as a function of implantation dose.

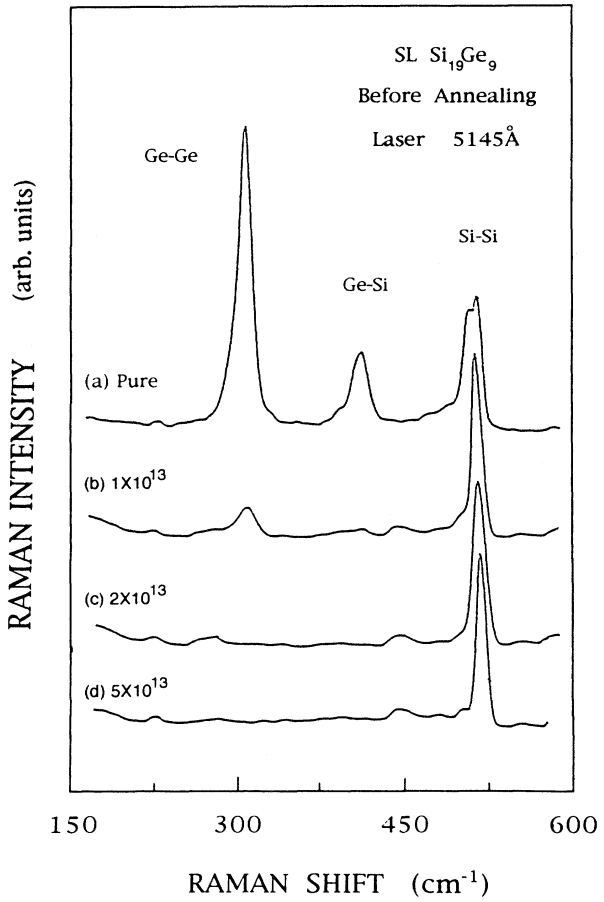

FIG. 8. Raman spectra of $Si_{19}Ge_9$, before annealing and before implantation with dose of (a) as grown, (b) 1×10^{13}, (c) 2×10^{13}, and (d) 5×10^{13} As ions cm^{-2}. The incident laser wavelength was 5145 Å.

ID $\geq 5\times10^{13}$ ions cm^{-2}.

In Fig. 7, we plot the intensity ratio between the Si-Si vibrations of Si_xGe_{1-x} and Si_yGe_{1-y} as a function of ID, which measures the degree of intermixing. The Si-Si vibration in Si_xGe_{1-x} arises when ID $=1\times10^{13}$ ions cm^{-2} and the two peaks cannot be distinguished when ID $\geq 3\times10^{13}$ ions cm^{-2}.

Figures 8 and 9 show the Raman spectra of the asymmetric $Si_{19}Ge_9$ SL excited by a 5145-Å laser line before and after the annealing, respectively, as a function of the implantation dose. Figure 8(a) shows the original SL's spectrum with the Ge and Si vibrations of 307, 409, 511, and 520 cm^{-1}. The difference between the two samples is a change in the frequencies of the Ge-Ge and Si-Si peaks, which depend on the strains in the layers. The thick buffer layer is essentially relaxed, so the strain on Ge and Si layers ϵ_{Ge} and ϵ_{Si} can be calculated. They are -1.45% and $+1.9\%$, respectively, for the $Si_{12}Ge_{12}$ SL, and -1.7% and $+1.17\%$, respectively, for the $Si_{19}Ge_9$ SL. The Ge layers are more strained in the $Si_{19}Ge_9$ than in the $Si_{12}Ge_{12}$ sample. The opposite is true for the Si layers.

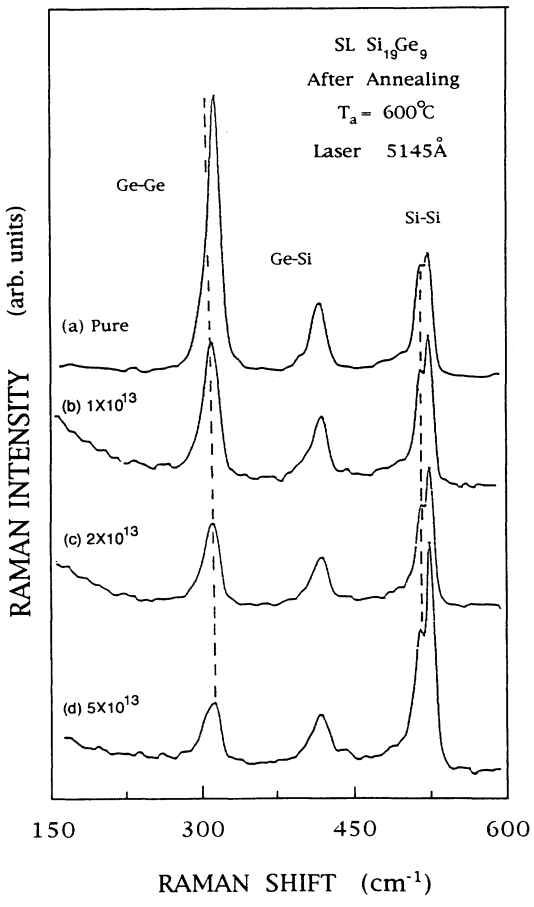

FIG. 9. Raman spectra of $Si_{12}Ge_{12}$ after As implantation and thermal annealing at 600 °C for 30 min with dose of (a) as grown, (b) 1×10^{13}, (c) 2×10^{13}, and (d) 5×10^{13} As ions cm^{-2}. The incident laser wavelength was 5145 Å.

Before annealing, the results are very similar to those obtained with the symmetrical $Si_{12}Ge_{12}$ SL. When the implantation dose is higher than 2×10^{13} ions cm^{-2}, the structure is destroyed and amorphization takes place [Figs. 8(b)–8(d)]. The unimplanted $Si_{19}Ge_9$ SL is not affected by the annealing of $T_a=600$ °C during $t_a=30$ min. The implanted and annealed samples are almost not affected by the implantation; a little strain release and intermixing of the Ge and Si layers can be observed, as one can see in Figs. 9(b)–9(d). The peaks are located at 304, 413, 513, and 520 cm^{-1}, their frequencies do not depend on the implantation dose. Intermixing in the $Si_{19}Ge_9$ sample can only be reached when the annealing conditions are much more drastic. When the annealing at $T=600$ °C for $3\frac{1}{2}$ h is followed by an annealing at $T=710$ °C for 30 min, we get a $Si_{0.5}Ge_{0.5}$ mixed crystal in the Ge layers and a thinner and more strained Si layer whose frequency is 510 cm^{-1}. When the symmetric and asymmetric SL's have been implanted with Ga or Ge, which have the same mass as As, but not the same valence, the same experimental results have been obtained for the same implantation doses. A kinetic model of the intermixing in $Si_{12}Ge_{12}$ and $Si_{19}Ge_9$ SL's is considered in Sec. IV.

IV. REORDERING AND DIFFUSION PROCESS DURING THERMAL ANNEALING

After implantation, the SL is damaged or even rendered amorphous when the ID is high enough. In addition, there is an interpenetration of Si and Ge atoms into the Ge and Si layers, respectively, which results in a partial inhomogeneous intermixing and in a release of stress between the Si and Ge layers. As a result, the annealing process in an implanted SL occurs in a material very different from the one before implantation. The first question to be asked is: does the intermixing take place in the damaged or amorphous medium or in the crystalline one? We shall then first calculate the time needed for recrystallization to take place. We shall compare the characteristic time of the reordering process with the annealing time, and then study the diffusion of Si (Ge) into the Ge (Si) layers in the symmetric $Si_{12}Ge_{12}$ SL and the asymmetric $Si_{19}Ge_9$ SL.

A. Fast ordering of the disordered Ge layers

We shall follow the approach suggested for the recrystallization of amorphous Si in Ref. 28. We have to distinguish between the recrystallization process in the disordered Ge and Si layers, which are governed by different activation energies and preexponential factors in the Arrhenius equation. The recrystallization of the Ge (Si) layers will be achieved when each atom makes a few diffusionlike jumps over energy barriers starting from its initial position to a new position in the media. The recrystallization rate coefficient is described by the Arrhenius equation:[28]

$$K_{RGe}=K_{0RGe}\exp\left[-\frac{\Delta E_{RGe}}{kT}\right] \tag{7}$$

which determines the frequency of ordering jumps of the same Ge atom during the thermal annealing. $K_{0R\mathrm{Ge}}$ is the preexponential factor, $\Delta E_{R\mathrm{Ge}}$ is the activation energy of the process, k is the Boltzmann constant, and $T=873$ K is the annealing temperature. The mean time between the two successive ordering jumps of the same Ge atom can be written

$$t_{R\mathrm{Ge}} \cong K_{R\mathrm{Ge}}^{-1} = t_{0R\mathrm{Ge}} \exp\left[\frac{\Delta E_{R\mathrm{Ge}}}{kT}\right], \tag{8}$$

where $t_{0R\mathrm{Ge}} = K_{0R\mathrm{Ge}}^{-1}$. An estimate of $t_{R\mathrm{Ge}}$ (or $K_{R\mathrm{Ge}}$) can be obtained from the self-diffusion coefficient of the Ge or Si atoms in the amorphous Ge:

$$D_{R\mathrm{Ge}} = D_{0R\mathrm{Ge}} \exp\left[-\frac{\Delta E_{R\mathrm{Ge}}}{kT}\right] \tag{9}$$

which is linked to $t_{R\mathrm{Ge}}$ by the following relations:[27,28]

$$t_{R\mathrm{Ge}} = \frac{\rho^2}{6D_{\mathrm{Ge}}} \quad \text{with} \quad t_{0R\mathrm{Ge}} \cong \frac{\rho^2}{6D_{0R\mathrm{Ge}}}, \tag{10}$$

where $\rho \cong d = 2.5$ Å is the average length of the atomic diffusion jump. The crystallization time $\tilde{t}_{R\mathrm{Ge}} \cong n_d t_{R\mathrm{Ge}}$ takes into account the fact that every Ge atom of the layer, experiences, on the average, n_d "ordering" jumps during $\tilde{t}_{R\mathrm{Ge}}$. For a rough estimate, we assume that $n_d \approx 5$ and $\tilde{t}_{R\mathrm{Ge}} \cong 5t_{R\mathrm{Ge}}$. The values of D_0 or ΔE for self-diffusion and interdiffusion of Ge and Si atoms in amorphous or crystalline Ge and Si materials are listed in Table I.

To calculate $t_{R\mathrm{Ge}}$ and $\tilde{t}_{R\mathrm{Ge}}$, one should take into account the variation of $\Delta E_{R\mathrm{Ge}}$, $D_{0\mathrm{Ge}}$, and $t_{0R\mathrm{Ge}}$ in time, corresponding to the structural changes during the recrystallization. However, this evolution of the diffusion parameters is unknown. That is why we limit ourselves to the calculation of the lower and upper time limits of $\tilde{t}_{R\mathrm{Ge}}$ for values of $\Delta E_{R\mathrm{Ge}}$ and $D_{R0\mathrm{Ge}}$ close to the diffusion parameters of the amorphous and crystalline Ge, respectively.

In the amorphous state, when the Arrhenius parameters are (Table I) $\Delta E_{R\mathrm{Ge}} = 1.6$ eV and $D_{R0\mathrm{Ge}} = 10^{-6}$ cm^2 s^{-1},[33] $t_{R\mathrm{Ge}}^{\min}$ can be estimated from Eqs. (8)–(10). At $T=873$ K, one finds that $t_{R\mathrm{Ge}}^{\min} \approx 0.18$ s and $\tilde{t}_{R\mathrm{Ge}}^{\min} \approx 1$ s. These time intervals are short compared to our experimental annealing time $t_a = 1.8 \times 10^3$ s.

In a state close to the crystalline Ge state, $t_{R\mathrm{Ge}}^{\max}$ can be estimated for the self-diffusion parameters of Ge in a crystalline Ge lattice[34] (Table I), $\Delta E_{R\mathrm{Ge}} = 3.07$ eV and $D_{R0\mathrm{Ge}} = 18.5$ cm^2 s^{-1}. From Eqs. (8)–(10), one finds that the time intervals $t_{R\mathrm{Ge}}^{\max} = 2.5$ s, and $\tilde{t}_{R\mathrm{Ge}}^{\max} = 12.5$ s are much shorter than the annealing time.

This implies that the Ge layer recrystallizes before intermixing or, in other words, that the diffusion of Si into the Ge layer occurs mainly in an ordered Ge layer.

B. Slow ordering of the disordered Si layers

The calculation of the crystallization time for the Si layer is quite similar to that made above for the Ge layer. We find here the lower limit $t_{R\mathrm{Si}}^{\min} \cong 25$ s, and $\tilde{t}_{R\mathrm{Si}}^{\min} \cong 10^2$ s, when we take into consideration the parameters for self-diffusion of Si in amorphous Si (see Table I). The upper limit, for self-diffusion of Si in crystalline Si, is $t_{R\mathrm{Si}}^{\max} \cong 2.5 \times 10^8$ s $\cong 8$ yr and $\tilde{t}_{R\mathrm{Si}}^{\max} \cong 40$ yr, much larger than our annealing time of $t_a \cong 30$ min.

These estimates show that the ordering in the disordered Si layer is slowed down by the rapid increase of the activation energy in the more ordered Si layer. Therefore interdiffusion of Ge atoms into the neighboring Si layers takes place mainly in a disordered material, contrary to what happens in the diffusion of Si atoms in the ordered Ge layer.

The effective activation energy ΔE_{Ge}^* of the interdiffusion of Ge atoms into the Si layer can be estimated from the following condition: During the experimental annealing time of $t_a = 0.5$ h, the material in the Si layer is ordered in part. Accordingly, the activation energy $\Delta E_{R\mathrm{Si}}$ for self-diffusion (and ordering) satisfies the following condition:

$$\tilde{t}''_{R\mathrm{Si}} \approx 5t''_{R\mathrm{Si}} = 0.5 \text{ h} = 1800 \text{ s}, \tag{11}$$

where

$$t''_{R\mathrm{Si}} \cong \frac{\rho^2}{6D''_{R\mathrm{Si}}} = \frac{\rho^2}{6D''_{R0\mathrm{Si}}} \exp\left[\frac{\Delta E''_{R\mathrm{Si}}}{kT}\right]. \tag{12}$$

Hence we find the activation energy of Si self-diffusion after some ordering in the Si layer during $t_a = 0.5$ h:

$$\Delta E''_{R\mathrm{Si}} = kT \ln\left[\frac{6D''_{R0\mathrm{Si}} t_a}{\rho^2}\right] \approx 2.7 \text{ eV} \tag{13}$$

for $D''_{R0\mathrm{Si}} \cong 10^{-3}$ cm^2 s^{-1}, $\rho^2 \cong 10^{-15}$ cm^2, and $t_a = 1800$ s.

The activation energy ΔE_{Ge}^* for the diffusion of Ge into Si is close to that of $\Delta E''_{R\mathrm{Si}}$ of the Si self-diffusion, i.e., $\Delta E_{\mathrm{Ge}}^* \cong \Delta E''_{R\mathrm{Si}} \cong 2.7$ eV.

Thus the diffusion coefficient of Ge into Si is governed by the diffusion coefficient

$$D_{\mathrm{Ge}=\mathrm{Si}}^* \cong 10^{-3} \exp\left[\frac{-2.7 \text{ eV}}{kT}\right] \mathrm{cm}^2 \mathrm{s}^{-1}. \tag{14}$$

Diffusion of Si into the Ge layers is characterized by the diffusivity

$$D_{\mathrm{Si}=\mathrm{Ge}}^* \cong 18.5 \exp\left[\frac{-3.07 \text{ eV}}{kT}\right] \mathrm{cm}^2 \mathrm{s}^{-1}, \tag{15}$$

since the diffusion parameters for this process are close to the parameters of Ge self-diffusion.

C. Mixing in the $Si_m Ge_n$ SL

The Ge and Si atoms have to reach the middle of the Si and Ge layers, respectively, or, in other words, have to diffuse through half of the layer's thickness. The corresponding mixing time is

$$t_{M\mathrm{Ge}} \cong \frac{(\Delta l_{\mathrm{Ge}}/2)^2}{D_{\mathrm{Si}=\mathrm{Ge}}^*} \quad \text{or} \quad t_{M\mathrm{Si}} \cong \frac{(\Delta l_{\mathrm{Si}}/2)^2}{D_{\mathrm{Ge}=\mathrm{Si}}^*}, \tag{16}$$

where $D_{\mathrm{Ge}=\mathrm{Si}}^*$ and $D_{\mathrm{Si}=\mathrm{Ge}}^*$ are defined by Eqs. (14) and

(15); $\Delta l_{Ge}=n\Delta d_{Ge}$, $\Delta l_{Si}=m\Delta d_{Si}$, and $\Delta d_{Si}\cong\Delta d_{Ge}\cong 1.4$ Å is the thickness of the atomic monolayers.

D. Diffusion in the symmetric SL, $m=n=12$

From Eq. (16), one finds $t_{MGe}\cong 167$ s, and $t_{MSi}\cong 8.6$ h. Therefore, if nothing prevents the intermixing, it would take much more time to mix the Si layer than the Ge one and, therefore, more Si atoms would move into the Ge layer than Ge atoms into the Si layers. However, this unbalanced interdiffusion cannot determine the intermixing in the diffusion fluxes of the Si and Ge atoms moving in the opposite directions, because an additional stress σ between adjacent layers is created. This stress, which balances the interdiffusion process, slows down the interdiffusion of the Ge atoms and/or increases the Si flux into the Ge layers, to equalize approximately the diffusion fluxes of Si and Ge atoms.

The value and direction of the interfacial stress σ which balances the diffusion fluxes are determined by the Le-Chatellier principle. The effective activation energies $\Delta\tilde{E}_{Si}$ and $\Delta\tilde{E}_{Ge}$ which govern the interdiffusion of Si and Ge atoms are modified by the stress between the adjacent layers:[35–38]

$$\Delta\tilde{E}_{Si}=\Delta E^*_{Si}+[\sigma\Delta V^*_{Si}] \quad \text{and} \quad \Delta\tilde{E}_{Ge}=\Delta E^*_{Ge}-[\sigma\Delta V^*_{Ge}] . \tag{17}$$

The stress σ increases (decreases) the activation energy for interdiffusion of Si (Ge) atoms into the Ge (Si) layers. Here ΔV^*_{Si} and ΔV^*_{Ge} are the activation volumes related to the diffusion of the Si and Ge atoms, which are usually close to the atomic volumes.

The effective stress-dependent interdiffusion coefficients can be written as follows:

$$\tilde{D}_{Si=Ge}\cong D^*_{0Si}\exp\left[-\frac{\Delta E^*_{Si}+(\sigma\Delta V^*_{Si})}{kT}\right], \tag{18}$$

$$\tilde{D}_{Ge=Si}\cong D^*_{0Ge}\exp\left[-\frac{\Delta E^*_{Ge}-(\sigma\Delta V^*_{Ge})}{kT}\right], \tag{19}$$

where the dependence of the prefactor on σ is neglected. The stress σ can be calculated from Eqs. (18) and (19) through the condition

$$\tilde{D}_{Si=Ge}\cong\tilde{D}_{Ge=Si} . \tag{20}$$

Hence we find

$$\sigma=\left[kT\ln\left[\frac{D^*_{0Si}}{D^*_{0Ge}}\right]-(\Delta E^*_{Si}-\Delta E^*_{Ge})\right]\times[\Delta V^*_{Si}+\Delta V^*_{Ge}]^{-1} . \tag{21}$$

Numerical estimations give $\sigma\cong 25$ kbar for $D_{0Si}\cong 10$ cm^2 s^{-1}, $D^*_{0Ge}\cong 10^{-3}$ cm^2 s^{-1}, $\Delta E^*_{Si}\cong 3$ eV, $\Delta E^*_{Ge}\cong 2.7$ eV, $\Delta V^*_{Si}\cong\Delta V^*_{Ge}\cong 1.3\times 10^{-23}$ cm^3, and $T=873$ K.

This stress reduces (enhances) the interdiffusion of Si (Ge) atoms by a factor of $\exp(\sigma\Delta V^*/kT)\cong 14.7$ and, as a result, the duration of intermixing in the symmetric SL under the influence of the stress σ becomes $\tilde{t}_{MSi}\cong\tilde{t}_{MGe}\cong 40$ min, in agreement with our experimental data.

E. Diffusion in the asymmetric SL $m=19$, $n=9$

There are marked differences between the two types of SL's. Here again the Ge layers will be ordered rapidly, but almost no recrystallization will take place in the thick Si layers. In addition, the thick Si layers impose a strain on the thin Ge layers which reduces interdiffusion of Ge atoms into the Si layers, which can only be partially mixed by the smaller amount of Ge atoms. From Eqs. (14)–(17), we see that without stress the mixing time for the Si layer in the asymmetric SL should be 2.5 times longer than in the symmetric SL, due to the larger thickness ($m'=19$) of the Si layers. Thus in the asymmetric SL, intermixing requires an annealing time substantially longer than our experimental one. A lower limit for intermixing in the presence of stress can be estimated by

$$t_A>t'_{MSi}\exp\left[-\frac{\sigma\Delta V^*}{kT}\right]\cong 1.5\text{h} . \tag{22}$$

This means that annealing during a few hours should lead to a partial asymmetrical intermixing of the SL. During our experimental annealing time of $t_a=30$ min at $T_a=873$ K, little interdiffusion took place in the asymmetric SL.

V. CONCLUSIONS

In the previous sections, we studied the disordering, the intermixing, and the crystallization processes of SL's composed of thin Si and Ge layers, which are induced by ion implantation at As doses of 1×10^{13}–1×10^{14} ions cm^{-2} and thermal annealing at $T=600$ °C for $t_a=30$ min. Two kinds of SL's were studied: the symmetric $Si_{12}Ge_{12}$ and the asymmetric $Si_{19}Ge_9$. With the help of TRIM computer cascade simulation, the effect of ion implantation was calculated. With the Raman-scattering technique, we monitored experimentally the created damage, the degree of intermixing, and the stress between the Si and Ge layers. A kinetic model was used to calculate the effect of the annealing process on the recrystallization and the intermixing processes. The main results specific to SL's composed of thin Si and Ge layers are the following.

(i) In addition to disordering, ion implantation partially intermixes the Si and the Ge layers (for a dose of 5×10^{13} ions cm^{-2}, intermixing reaches 5–10 %).

(ii) When the SL's have been rendered amorphous by ion implantation, thermal annealing at 600 °C for 30 min completely intermixes the symmetric $Si_{12}Ge_{12}$ SL but only releases some stress in the asymmetric $Si_{19}Ge_9$ one. These effects depend on the implantation dose.

(iii) After ion implantation and thermal annealing, Si diffuses into the crystalline Ge layers, but Ge diffuses in mainly disordered Si layers, since the recrystallization of Ge (Si) requires a short (long) time compared to 30 min. In the symmetric SL, diffusion and intermixing are

strongly enhanced by ion implantation, but in the asymmetric SL these processes are much slower than in the symmetric one and complete intermixing is reached under more severe conditions. The proposed model shows that interfacial stress plays an important role in the interdiffusion and intermixing processes.

(iv) Our model explains the influence of the layer thickness and stress on the intermixing. It shows that substantial intermixing can be obtained at a moderate temperature during a relatively short time.

ACKNOWLEDGMENTS

This work has been made possible by Volkswagen Stiftung contract and by a Deutsche Technion Gesellschaft e.V fund.

[1]M. D. Camras, N. H. Holonyak, Jr., R. D. Burnham, W. Streifer, D. R. Scifres, T. L. Pauli, and C. Lindström, J. Appl. Phys. **54**, 5637 (1983).

[2]K. Meehan, J. M. Brown, P. Gavrilovic, N. Holonyak, Jr., R. D. Burnham, T. L. Pauli, and W. Streifer, J. Appl. Phys. **55**, 2672 (1984).

[3]R. L. Thornton, R. D. Burnham, T. L. Pauli, N. Holonyak, Jr., and D. G. Deppe, Appl. Phys. Lett. **49**, 133 (1986).

[4]R. L. Thornton, D. F. Welch, R. D. Burnham, T. L. Pauli, and P. S. Cross, Appl. Phys. Lett. **49**, 157 (1986).

[5]W. D. Laidig, N. Holonyak, Jr., R. D. Camras, K. Hess, J. J. Coleman, P. D. Dapkin, and J. Bardeen, Appl. Phys. Lett. **38**, 776 (1981).

[6]B. Tell, B. C. Johnson, J. L. Zyvkind, J. R. Brown, J. W. Sulhoff, K. F. Brown-Goebler, B. I. Miller, and U. Koren, Appl. Phys. Lett. **52**, 1428 (1988).

[7]T. Venkatesan, S. A. Schwarz, D. M. Hwang, R. Bhat, M. Koza, H. W. Yoon, P. Mei, Y. Arakawa, and A. Yariv, Appl. Phys. Lett. **49**, 701 (1986).

[8]S. Yu, T. Y. Tan, and U. Gösele, J. Appl. Phys. **69**, 3547 (1991).

[9]P. Gavrilovic, D. G. Teppe, K. Meehan, N. Holonyak, Jr., J. J. Coleman, and R. D. Burnham, Appl. Phys. Lett. **47**, 130 (1985).

[10]U. Gnutzman and K. Clausecker, Appl. Phys. Lett. **3**, 9 (1974).

[11]S. Satpathy, R. M. Martin, and C. G. Van de Walle, Phys. Rev. B **38**, 13 237 (1988).

[12]T. P. Pearsall, J. R. Vandenberg, R. Hull, and J. R. Brown, Phys. Rev. Lett. **63**, 2104 (1989).

[13]R. Zachai, K. Eberl, G. Abstreiter, E. Kasper, and H. Kibbel, Phys. Rev. Lett. **64**, 1055 (1990).

[14]H. Okumura, K. Miki, S. Misawa, K. Sakamoto, T. Sakamoto, and S. Yoshida (unpublished).

[15]J. P. Noël, J. E. Greene, N. L. Rowell, S. Kechang, and D. C. Houghton, Appl. Phys. Lett. **55**, 1525 (1989).

[16]J. P. Noël, J. E. Greene, N. L. Rowell, and D. C. Houghton, Appl. Phys. Lett. **56**, 265 (1990).

[17]S. J. Chang, K. L. Wang, R. C. Bowman, Jr., and P. M. Adams, Appl. Phys. Lett. **54**, 1253 (1989).

[18]D. C. Houghton, C. J. Gibbings, C. J. Tuppen, M. H. Lyons, and M. A. G. Halliwell, *Thin Solid Films* **183**, 171 (1989).

[19]S. M. Hu, D. C. Ahlgren, P. A. Ronsheim, and J. O. Chu, Phys. Rev. Lett. **67**, 1450 (1991).

[20]S. M. Prokes, O. J. Glembocki, and D. J. Godbey, Appl. Phys. Lett. **60**, 1087 (1992).

[21]W. Freiman, R. Beserman, K. Dettmer, and F. R. Kessler, Appl. Phys. Lett. **60**, 1673 (1992).

[22]J. F. Ziegler, J. P. Biersack, and U. Littmer, *The Stopping and Range of Ions in Solids* (Pergamon, New York, 1985), Vol. I.

[23]J. W. Mayer, L. Eriksson, and J. A. Davis, *Ion Implantation in Semiconductors, Silicon and Germanium* (Academic, New York, 1970).

[24]M. W. Thompson, *Defects and Radiation Damage in Metals* (Cambridge University Press, Cambridge, England, 1969).

[25]G. Carter and J. S. Colligon, *Ion Bombardment on Solids* (Menman, London, 1968).

[26]J. M. Poate, in *Amorphous Silicon and Related Materials,* edited by K. Fritsche (World Scientific, Singapore, 1988).

[27]Yu. L. Khait, R. Brener, and R. Beserman, Phys. Rev. B **38**, 6107 (1988).

[28]Yu. L. Khait and R. Beserman, Phys. Rev. B **33**, 2983 (1986).

[29]Yu. L. Khait, J. Salzman, and R. Beserman, Appl. Phys. Lett. **53**, 2135 (1988).

[30]I. Abdulhalim, R. Beserman, Yu. L. Khait, and R. Weil, Appl. Phys. Lett. **51**, 1898 (1987).

[31]W. Koschinski, K. Dettmer, and F. K. Kessler, J. Appl. Phys. **72**, 471 (1992).

[32]M. A. Renucci, J. B. Renucci, and M. Cardona, in *Proceedings of the Second International Conference on Light Scattering in Solids,* edited by M. Balkanski (Flammarion, Paris, 1971), p. 326.

[33]S. M. Prokes and F. Spaepen, Appl. Phys. Lett. **47**, 234 (1985).

[34]R. G. Borg and G. J. Dones, *An Introduction to Solid State Diffusion* (Academic, New York, 1990).

[35]G. A. Samara, in *Solid State Physics,* edited by H. Ehrenreich and D. Turnbull (Academic, New York, 1984), Vol. 38, p. 1.

[36]Yu. L. Khait, Phys. Rep. **99**, 237 (1983).

[37]Yu. L. Khait, J. Salzman, and R. Beserman, Appl. Phys. Lett. **55**, 1170 (1989).

[38]D. Lazarus, in *Diffusion in Body-Centered Metals,* edited by J. A. Weeler and F. R. Winslow (American Society for Metals, Metals Park, OH, 1965).

[39]S. Hayashi, H. Wakayama, T. Okada, S. S. Kim, and K. Yamamoto, J. Phys. Soc. Jpn. **56**, 243 (1987).